Quantitative insights into the role of gravitational collapse in major orogenic belts

Marcello Viti, Dario Albarello and Enzo Mantovani
Dipartimento di Scienze della Terra, Università degli Studi di Siena, Italy

Abstract
Previous works have proposed gravitational collapse as the driving mechanism of extensional deformation of thickened continental crust. In this work we investigate the physical plausibility of this interpretation for the most important orogenic belts of the world by computing the spreading force induced by lateral variations of crustal thickness and the possible resisting forces. Two collapse mechanisms, one involving the upper crust only and the other the whole crust, have been considered. Particular attention has been devoted to constrain the uncertainty affecting such computations, mostly due to the large variability of the thermal and mechanical properties of rocks. The results obtained show that gravitational collapse is not a plausible mechanism in the four Mediterranean orogens here considered (Northern Apennines, Calabrian Arc, Hellenic Arc and Carpathians). For the other orogenic zones we have taken into account (Western US Cordillera, Central Andes, Himalayas and Central Alps) the large uncertainty that affects the estimate of spreading and resisting forces does not allow to firmly assess the feasibility of gravitational collapse.

Key words *gravitational collapse – rheology of the crust – tectonic forces – continental crust – lithospheric stress*

1. Introduction

Gravitational collapse of thickened continental crust has often been invoked as a possible driving mechanism of the extensional deformation observed in orogenic domains such as the Western European Variscides, North America Cordillera, Central Andes, Tibetan Plateau, Alps, Northern Apennines and Aegean region (*e.g.*, Dalmayer and Molnar, 1981; Dewey, 1988; Harry *et al.*, 1993; Carmignani *et al.*, 1994; Eva and Solarino, 1998; Gautier *et al.*, 1999; Vanderhaeghe and Teyssier, 2001).

However, in several cases the plausibility of the collapse model has been questioned and alternative driving mechanisms have been proposed (*e.g.*, Isacks, 1988; Peltzer and Saucier, 1996; Henk, 1999; Mantovani *et al.*, 2001, 2002, 2006; Bird, 2002). This suggests that the mere evidence of extensional deformation within an orogenic belts does not necessarily imply that gravitational spreading is the driving mechanism. In fact, most of the above-mentioned interpretations arbitrarily assume the collapse of thickened crust as feasible, independently of the related structural/tectonic context and quantitative analysis of relevant tectonic forces. However, analytical computations and numerical simulations have shown that the strength of a thickened belt may overcome the spreading force induced by lateral variations of crustal thickness (*e.g.*, Liu, 2001) and that the strength of the foreland facing the belt may considerably contribute to maintain

Mailing address: Dr. Marcello Viti, Dipartimento di Scienze della Terra, Università degli Studi di Siena, Via Laterina 8, 53100 Siena, Italy; e-mail: vitimar@unisi.it

large-scale gradients of crustal thickness and topographic relief (*e.g.*, England and Houseman, 1988; Maggi *et al.*, 2000; Rey *et al.*, 2001).

The above considerations suggest that the feasibility of the collapse model in a given zone should be checked by properly estimating driving and resisting forces. However, this check is not an easy task due to the still incomplete knowledge of the structural, thermal and mechanical properties of the continental lithosphere. The large variability of the continental crust, in terms of its lithological composition, may cause considerable uncertainty on the depth distribution of crustal density, which in turn affects the estimate of the gravitational spreading force. An example in this sense is provided by the debate about the mechanism of gravitational collapse which would have generated the Great Basin (southwestern U.S.A.) in early Cenozoic (*e.g.*, Jones *et al.*, 1999; Rey and Costa, 1999). Analogously, the assessment of the force that resists gravitational collapse is affected by many uncertainties, most of them related to the still limited knowledge of the mechanical behaviour of the crust-mantle system. For instance, the strength of upper and lower crustal layers is a matter of lively debate, due to the large variability of the rheological parameters of rocks and lithospheric geotherms (Burov, 2003; Ranalli, 2003). Overlooking these sources of uncertainty compromises the reliability of the estimate of the tectonic forces responsible for gravitational collapse.

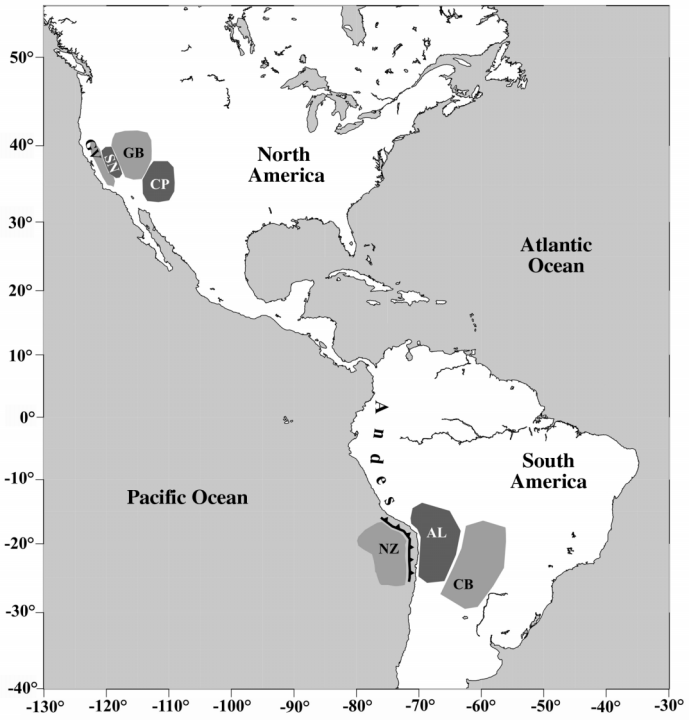

Fig. 1a. Geographical location of some orogenic systems considered in this study. For each system, the mountain belt (dark grey), the underthrusting plate and the foreland zone (both light grey) are shown. Toothed lines indicate subduction or thrust boundaries. Abbreviations refer to the tectonic domains whose structural and thermal parameter are reported in table I. a) North and South America. Western United States Cordillera: CP=Colorado Plateau; GB=Great Basin; GV=Great Valley; SN=Sierra Nevada. Central Andes: AL=Altiplano Plateau; CB=Chaco Basin; NZ=Nazca Plate.

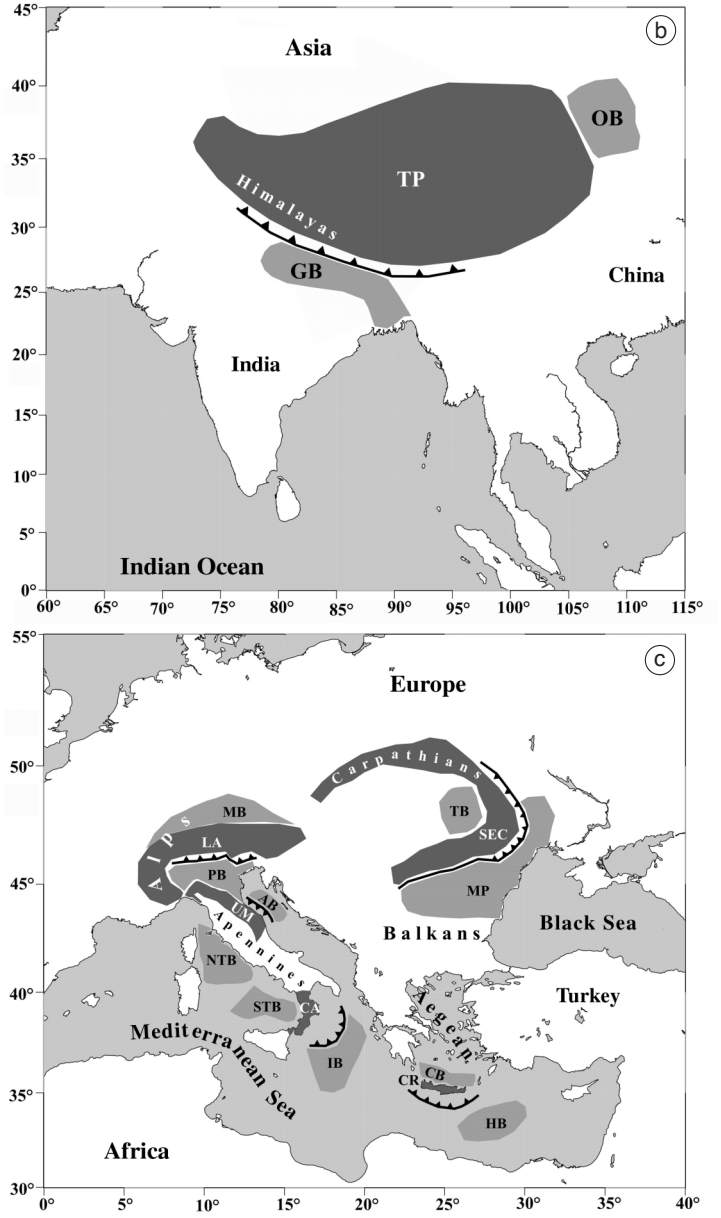

Fig. 1b,c. Geographical location of some orogenic systems considered in this study. For each system, the mountain belt (dark grey), the underthrusting plate and the foreland zone (both light grey) are shown. Toothed lines indicate subduction or thrust boundaries. Abbreviations refer to the tectonic domains whose structural and thermal parameter are reported in table I. b) Himalayas: GB=Gange Basin; OB=Ordos Basin; TP=Tibetan Plateau. c) Mediterranean region. Central Alps: LA=Lepontine Alps; MB=Molasse Basin; PB=Po Basin. Northern Apennines: AB=Adriatic Basin; NTB=Northern Tyrrhenian Basin; UM=Umbria-Marche Apennines. Calabrian Arc: CA=Calabria; IB=Ionian Basin; STB=Southern Tyrrhenian Basin. Hellenic Arc: CB=Cretan Basin; CR=Crete; HB=Herodotus Basin. Carpathians: MP=Moesian Platform; SEC=Southeastern Carpathians; TB=Transylvanian Basin.

The aim of this work is providing quantitative insights into this problem, by computing the force balance for eight major orogenic belts in the world: Western US Cordillera, Central Andes, Himalayas, Central Alps, Northern Apennines, Calabrian Arc, Hellenic Arc and Carpathians (fig. 1a-c). The structural and thermal data available for each belt, along with the related uncertainties (table I), have been used to obtain realistic ranges of driving and resisting forces, which allow investigating the role of gravitational collapse in active extension.

Table I. Structural and thermal data concerning the 8 orogenic systems considered in this study. The first, second and third row for each zone refer to the subducting crust, the chain and the foreland, respectively. The second box (Western US Cordillera 2) only includes two rows, which are respectively referred to the chain and the foreland. See fig. 1a-c for geographical location of the various domains. e = average height of the chain above the surrounding domain; L = length of the underthrusting boundary; h_W, h_{UC}, h_{LC} = thickness of the water layer, upper crust and lower crust, respectively; q_0 = surface heat flow. Small letters close to numbers indicate the reference. For each zone of the various orogenic systems only the parameters which are relevant for the computation of spreading and resisting forces acting at that zone (F, R and T at subduction boundaries and F, R and C at non-subduction ones) are reported. See text for explanations.

Zone	e km	h_W km	h_{UC} km	h_{LC} km	q_0 (mW·m^{-2})	References
Western US Cordillera 1						
Great Valley	-	-	15[a,b]	15[a,b]	25-55[c]	[a] Fliedner *et al.* (2000)
Sierra Nevada	3.5	-	20[b,d]	24[b,d]	40-57[e]	[b] Ruppert *et al.* (1998)
Great Basin	1.5	-	18[b,f]	12[b,f]	59-125[e]	[c] Wang and Munroe (1982)
						[d] Smith and Bruhn (1984)
						[e] Harry *et al.* (1993)
						[f] Satarugsa and Johnson (2000)

Zone	e km	h_W km	h_{UC} km	h_{LC} km	q_0 (mW·m^{-2})	References
Western US Cordillera 2						
Great Basin	1.5	-	18[a,b]	12[a,b]	59-125[c]	[a] Ruppert *et al.* (1998)
Colorado Plateau	2.5	-	25[a,d,e]	15[a,d,e]	42-94[a,d,e]	[b] Satarugsa and Johnson (2000)
						[c] Harry *et al.* (1993)
						[d] Hinojosa and Mickus (2002)
						[e] Lowry and Smith (1995)

Zone	e km	L km	h_W km	h_{UC} km	h_{LC} km	q_0 (mW·m^{-2})	References
Central Andes							
Nazca Plate	-	150[a]	5[b]	-	7[b]	-	[a] Giese *et al.* (1999)
Altiplano	5.	-	-	23[c]	45[c]	70-130[d]	[b] Flueh *et al.* (1998)
Chaco Basin	-	-	-	28[b,e]	10[b,e]	40-50[d]	[c] Schmitz *et al.* (1999)
							[d] Springer and Förster (1998)
							[e] Lucassen *et al.* (2001)

Zone	e km	L km	h_{UC} km	h_{LC} km	q_0 (mW·m^{-2})	References
Himalayas						
Gange Basin	-	160[a]	15[b]	25[b]	-	[a] Kayal (2001)
Tibetan Plateau	5.	-	24[c]	46[c]	58-106[c,d]	[b] Cattin *et al.* (2001)

Table I (*continued*)**.**

Zone	e km	L km	h_{UC} km	h_{LC} km	q_0 (mW·m^{-2})	References
Himalayas						
Ordos Basin	1.	-	19[(c)]	24[(c)]	48-72[(c,d)]	[(c)] Wang (2001) [(d)] Hu *et al.* (2000)

Zone	e km	L km	h_{UC} km	h_{LC} km	q_0 (mW·m^{-2})	References
Central Alps						
Po Basin	-	125[(a,b)]	20[(a)]	10[(a)]	-	[(a)] Okaya *et al.* (1996)
Lepontine Alps	2.5	-	30[(a,b,c)]	30[(a,b,c)]	60-80[(d)]	[(b)] Marchant and Stampfli (1997)
Molasse Basin	0.5	-	20[(a,b)]	10[(a,b)]	68-110[(c)]	[(c)] Cermak and Bodri (1996) [(d)] Della Vedova *et al.* (1995)

Zone	e km	L km	h_{UC} km	h_{LC} km	q_0 (mW·m^{-2})	References
Northern Apennines						
Adriatic Basin	-	100[(a)]	20[(b)]	10[(b,c)]	-	[(a)] Ponziani *et al.* (1995)
Umbria-Marche Belt	1.	-	15[(a,d,e)]	20[(a,d,e)]	40-60[(f, g)]	[(b)] Okaya *et al.* (1996)
N. Tyrrhenian Basin	-	-	12[(e)]	10[(e)]	67-147[(f)]	[(c)] Finetti *et al.* (2001) [(d)] Giudici and Gualteri (1998) [(e)] Gualteri *et al.* (1998) [(f)] Della Vedova *et al.* (1995) [(g)] Pasquale *et al.* (1997)

Zone	e km	L km	h_W km	h_{UC} km	h_{LC} km	q_0 (mW·m^{-2})	References
Calabrian Arc							
Ionian Sea	-	120[(a)]	4[(a,b)]	7[(a,b)]	8[(a,b)]	-	[(a)] Van Dijk *et al.* (2000)
Calabria	1.	-	-	20[(a)]	6[(a)]	40-60[(c)]	[(b)] De Voogd *et al.* (1992)
S. Tyrrhenian Basin	-	-	4[(a,d)]	-	10[(a,d)]	75-143[(e)]	[(c)] Cataldi *et al.* (1995) [(d)] Duschenes *et al.* (1986) [(e)] Della Vedova *et al.* (1995)

Zone	e km	L km	h_W km	h_{UC} km	h_{LC} km	q_0 (mW·m^{-2})	References
Hellenic Arc							
Herodotus Basin	-	150[(a)]	3[(a,b)]	10[(a,b)]	11[(a,b)]	-	[(a)] Bohnhoff *et al.* (2001)
Crete	1.5	-	-	13[(a)]	20[(a)]	50-60[(c)]	[(b)] De Voogd *et al.* (1992)
Cretan Basin	-	-	2[(a)]	6[(a)]	8[(a)]	60-70[(c)]	[(c)] Cermak (1993)

Zone	e km	L km	h_{UC} km	h_{LC} km	q_0 (mW·m^{-2})	References
Carpathians						
Moesian Platform	-	180[(a)]	14[(b)]	16[(b)]	-	[(a)] Linzer *et al.* (1998)
Southeastern Carpathians	1	-	20[(b)]	30[(b)]	50-70[(b)]	[(b)] Fan *et al.* (1998) [(c)] Andreescu *et al.* (2002)
Transylvanian Basin	0.5	-	12[(b,c)]	18[(b,c)]	40-60[(b,c,d)]	[(d)] Serban *et al.* (2001)

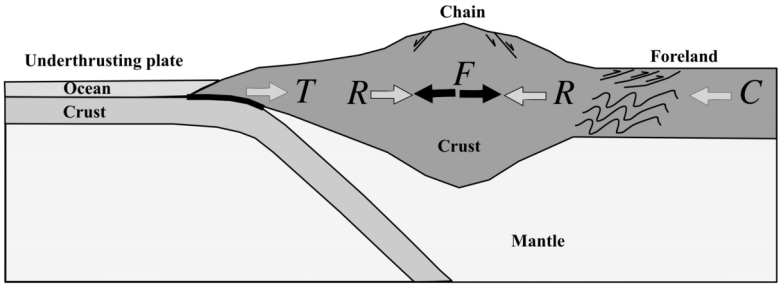

Fig. 2. Driving (solid arrows) and resisting (empty arrows) forces presumably involved in the gravitational collapse of a thickened crust. F=gravitational spreading force; R=tensional strength of the chain; C=compressional strength of the foreland; T=frictional resistance at the underthrusting boundary (thick line), whose length is L in the text.

2. Dynamics of gravitational collapse

It has been demonstrated that a lateral variation of crustal thickness produces a spreading force, whereas thickening of the underlying lithospheric mantle generates an opposite effect (Rey *et al.*, 2001). An upper bound for the spreading force can therefore be obtained by considering the difference in crustal thickness between the chain and the related foreland (*e.g.*, Liu and Shen, 1998; Liu, 2001; Liu and Yang, 2003).

Assuming that the spreading force only acts in the crust, the collapse of a thickened belt requires that the crust is decoupled from the lithospheric mantle by a zone of low mechanical strength, as revealed by rheological profiles of continental lithosphere (*e.g.*, Bird, 1991; Viti *et al.*, 1997; Meissner and Mooney, 1998). In our computations, we have adopted a structural scheme involving a thickened crustal domain confined by a thinner foreland, on one side, and by a subduction or collision boundary, on the other (fig. 2). The spreading force (F) generated in the thickened crust is resisted by the tensional strength of the chain (R), the compressional strength of the foreland (C) and the frictional resistance at the underthrusting boundary (T).

Gravitational collapse can only occur when the spreading force overcomes the strength of the chain (*e.g.*, Liu, 2001): $F-R\geq 0$. However, this condition is not sufficient, due to the contribution of the other boundary resistances. In particular, lateral collapse towards the foreland occurs when

$$F-(R+C)\geq 0 \qquad (2.1a)$$

and towards the underthrusting boundary when

$$F-(R+T)\geq 0\,. \qquad (2.1b)$$

In the next we describe the formulation adopted for estimating the above driving and resisting forces.

2.1. *Spreading force*

The gravitational spreading force is induced by the horizontal gradient of potential energy stored in the crust of the orogenic and foreland domains, which depends on the lateral variations of crustal thickness and density (*e.g.*, Molnar and Lyon-Caen, 1988). Various mechanisms of gravitational collapse, involving different portions of the crust, have been discussed (*e.g.*, Rey *et al.*, 2001). In this work, we have investigated both the possibilities that the collapse is confined to the upper crust and that it involves the whole crust. In these cases, lateral spreading would be allowed by low-strength layers respectively at the base of the upper and lower crust, as predicted by strength envelopes (*e.g.*, Meissner and Mooney, 1998).

For the simplified structural model shown in fig. 3 the average spreading force (F) per unit length of the orogenic belt (Nm^{-1}) is given by (*e.g.*, Coblentz and Sandiford, 1994; Liu, 2001)

$$F = \int_{-e}^{z_C} \Delta p(z)\,\mathrm{d}z \qquad (2.2a)$$

$$\Delta p(z) = g \int_{-e}^{z} \left[\rho_C(\zeta) - \rho_F(\zeta)\right]\mathrm{d}\zeta \qquad (2.2b)$$

where Δp is the difference of lithostatic pressure in the chain and foreland, ρ_C and ρ_F are the related depth-distributions of rock density and g is the gravity acceleration (9.81 ms^{-2}). e is the topographic height of the chain above the foreland, z is the depth measured downward from the top of the foreland and z_C is the the depth of the bottom of the collapsing crustal layer. It follows from fig. 3 that $z_C = h_{CU}$ for collapse of the upper crust, and $z_C = h_{CU} + h_{CL}$ for collapse of the whole crust.

The above computation of F applies to both cases of gravitational collapse shown in fig. 1a-c, *i.e.* towards the foreland or towards the subducting plate. The structural data about foreland, chain and subducting plate, required to estimate F by eq. (2.2a), are reported in table I, for each of the orogenic systems considered.

2.2. *Strength of the chain and the foreland*

The integrated tensional strength of the thickened crust of the chain (Nm^{-1}) is defined by (*e.g.*, Liu and Shen, 1998; Liu, 2001)

$$R = \int_{-e}^{z_C} \Delta\sigma_T(z)\,\mathrm{d}z \qquad (2.3a)$$

where $\Delta\sigma_T(z)$ is the depth-distribution of the tensional strength of the orogenic belt and z_C is defined as in eq. (2.2a). Analogously, the compressional strength of the foreland is defined by

$$C = \int_{0}^{z_F} \Delta\sigma_C(z)\,\mathrm{d}z \qquad (2.3b)$$

where $\Delta\sigma_C(z)$ is the depth-distribution of the compressional strength. The depth z_F corresponds to the bottom of the crust of the foreland opposing collapse and depends on the collapse mechanism considered (upper or whole crust; $h_{FU} \leq z_F \leq h_{FU} + h_{FL}$ from fig. 3). C represents a lower bound for the strength of the foreland, since it does not take into account the contribution of the mantle facing the crustal root of the chain.

To evaluate R and C, constitutive equations, describing the inelastic deformation of rocks, have to be adopted (Kohlstedt *et al.*, 1995). In computing classical strength envelopes (Goetze and Evans, 1979), two basic deformation mechanisms, *i.e.* frictional slip on optimally oriented faults (in the brittle field) and dislocation creep (in the crystal plastic field) are taken into account. However, a large amount of experimental results,

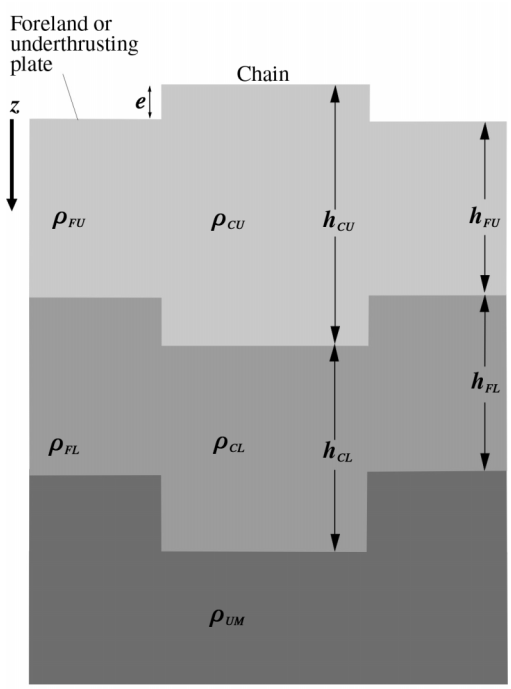

Fig. 3. Schematic structural model used in computations of spreading force and resistances. Light, medium and dark gray depicts upper crust, lower crust and upper mantle, respectively. ρ_{UM} = density of the upper mantle; ρ_{CU}, ρ_{CL} (ρ_{FU}, ρ_{FL}) = density of the upper and lower crust in the chain (foreland); h_{CU}, h_{CL} (h_{FU}, h_{FL}) = thickness of the upper and lower crust in the chain (foreland); e = topographic height of the chain above the foreland; z = depth.

concerning high-pressure rock deformation (Ord, 1991; Shimada, 1993), suggests that a third kind of behaviour, often indicated as semi-brittle yielding, should be considered. This behaviour involves several kinds of micro-mechanisms, ranging from high-pressure fracture to true plasticity. Within the depth range where semi-brittle deformation dominates, rock strength becomes nearly independent of depth and stress regime, although it depends on rock composition.

2.3. *Frictional slip, semi-brittle deformation and plastic flow*

We assume that the rock strength at a given depth is the minimum value among the stress differences required to drive frictional slip, semi-brittle deformation and plastic flow ($\Delta\sigma_{FR}$, $\Delta\sigma_{SB}$ and $\Delta\sigma_{PL}$, respectively)

$$\Delta\sigma = \min(\Delta\sigma_{FR}, \Delta\sigma_{SB}, \Delta\sigma_{PL}) \qquad (2.4)$$

where $\Delta\sigma=\sigma_1-\sigma_3$ and σ_1, σ_3 are the maximum and minimum principal stresses, respectively. In the extensional (compressional) Andersonian stress regime σ_1 is vertical (horizontal), *e.g.* Jaeger and Cook (1984).

Frictional strength of faults linearly depends on the lithostatic and pore fluid pressure (p and p_f, respectively) by the relationship

$$\Delta\sigma_{FR} = ap_e + b \qquad (2.5)$$

where $p_e=p-p_f$ is the effective pressure and the coefficients a and b depend on the friction coefficient and tectonic stress regime (Jaeger and Cook, 1984). In particular, the estimate of the mechanical strength of the chain and foreland by eqs. ((2.3a) and (2.3b)) requires the computation of $\Delta\sigma_{FR}$ in the tensional and the compressional stress regime, respectively. Realistic values of the coefficients a and b in eq. (2.5) can be obtained for the above stress regimes by taking into account Byerlee's (1978) laws on rock friction. For the tensional regime, Mueller *et al.*'s (1996) formulation gives $a=0.79$ and $b=0$ in the range $0<p_e<529$ MPa, and $a=0.68$ and $b=57$ MPa for $p_e>529$ MPa, while for the compressional regime $a=3.68$ and $b=0$ when $0<p_e<113$ MPa, and $a=2.12$ and $b=177$ MPa for $p_e>113$ MPa.

Since the relatively large permeability of lithospheric rocks suggests that the long-term pore pressure is close to hydrostatic values (Zoback and Townend, 2001), in computing $\Delta\sigma_{FR}$ by eq. (2.5) we have assumed that p_f always corresponds to the hydrostatic pressure and $p_e=g(\rho-\rho_W)z$, where $\rho_W=1000$ kg m^{-3} is the water density.

Since no reliable constitutive law for the semi-brittle regime is currently available, the related rock strength is considered pressure-independent and affected by lithological composition only. Tentative values of $\Delta\sigma_{SB}$ for the upper and lower crust are assumed to be 400 MPa and 300 MPa, respectively (Shimada, 1993; Bassi, 1995).

A power law related to steady-state dislocation creep is commonly adopted to describe the high-temperature, plastic deformation of silicates (Weertman, 1978; Poirier, 2005)

$$\Delta\sigma_{PL} = \left(\frac{\dot{\varepsilon}}{A}\right)^{1/n} e^{H/nRT} \qquad (2.6)$$

where $\dot{\varepsilon}$, T, n, H, A, R are strain rate, absolute temperature, stress exponent, activation energy, pre-exponential coefficient and the gas constant (8.31 J°K^{-1}mol^{-1}), respectively. Although the flow strength $\Delta\sigma_{PL}$ generally increases from upper to lower crustal rocks, the values of the rheological parameters n, H, and A strongly vary with rock composition and water content (*e.g.*, Fernàndez and Ranalli, 1997). Moreover, the lithological characterization of the crust by seismic surveys is not unequivocal, due to the complex relationships among mineralogical composition, thermal state and velocity of seismic waves (Christensen and Mooney, 1995). Considering the above problems, we have assumed that the flow strength of the upper and lower crust may vary between a lower and upper bound, respectively related to the weakest and strongest crustal rock type (tables II and III).

Geological structural data indicate that tectonic strain rate may vary in a large interval: 10^{-17}-10^{-11} s^{-1} (Pfiffner and Ramsay, 1982). However, estimates of seismic deformation and geodetic measurements (*e.g.*, Talwani, 1999) suggest that this range may be narrower (10^{-16}-10^{-15}

Table II. Parameterisation of the crust and mantle used in computations. ρ = density; k = thermal conductivity; Q = heat production per unit volume; $\Delta\sigma_{SB}$ = semi-brittle strength; A = pre-exponential factor; n = stress exponent; H = activation energy, τ = fault shear strength. See text for details. Small letters close to numbers indicate the relevant references.

Layer	ρ (kg m^{-3})	k (W m^{-1} °C^{-1})	Q (μW m^{-3})	$\Delta\sigma_{SB}$ (MPa)	Rock type	A (MPa^{-n} s^{-1})	n	H (kJ mol^{-1})
Upper crust	2600-2800[a]	2.4-3.8[c]	1.0-2.5[d]	400[e]	Westerly granite (wet)[f]	0.0002	1.9	141
					Quartz-diorite (wet)[f]	0.032	2.40	219
Lower crust	2800-3000[a]	2.6-3.5[c]	0.05-0.5[d]	300[e]	Anorthosite (wet)[g]	0.00032	3.2	238
					Maryland diabase (dry)[h]	0.063	3.1	276
Upper mantle	3200-3300[b]	3.7-4.6[c]	0.001-0.01[d]	600[e]	Anita Bay dunite (wet)[i]	10000.	3.4	445
					Anita Bay dunite (dry)[i]	32000.	3.6	535

τ (MPa)	Subduction fault	Continental thrust
	14-43[l]	25-50[m]

[a] Okaya *et al.* (1996); [b] Jones *et al.* (1998); [c] Lowry and Smith (1995); [d] Ranalli (1997); [e] Bassi (1995); [f] Hansen and Carter (1982); [g] Shelton and Tullis (1982); [h] Caristan (1982); [i] Chopra and Paterson (1984); [l] Tichelaar and Ruff (1993); [m] England and Molnar (1991).

Table III. Bounding values for the various physical parameters, which has been adopted to assess the uncertainty that may affect the crustal spreading force and the mechanical strength of crust and upper mantle. *LD*, *HD* = «Low Density» and «High Density» models. *LS*, *HS* = «Low Strength» and «High Strength» models. *UC*, *LC*, *UM* = Upper Crust, Lower Crust and Upper Mantle. Other symbols as in table II. See text for explanations.

Density (kg m^{-3})	Spreading force *LD*	*HD*
ρ_{UC}, ρ_{LC} (chain)	2600, 2800	2600, 3000
ρ_{UC}, ρ_{LC}, ρ_{UM} (foreland)	2600, 3000, 3300	2600, 2800, 3200
Parameter	**Mechanical strength *LS***	***HS***
$\dot{\varepsilon}$ (s^{-1})	10^{-16}	10^{-15}
q_0 (mW m^{-2})	Max in table I	Min in table I
k_{UC}, k_{LC}, k_{UM} (W m^{-1} °C^{-1})	2.4, 2.6, 3.7	3.8, 3.5, 4.6
Q_{UC}, Q_{LC}, Q_{UM} (μW m^{-3})	2.5, 0.5, 0.01	1.0, 0.05, 0.001
A_{UC}, A_{LC}, A_{UM} (MPa^{-n} s^{-1})	0.0002, 0.00032, 10000	0.032, 0.063, 32000
n_{UC}, n_{LC}, n_{UM}	1.9, 3.2, 3.4	2.4, 3.1, 3.6
H_{UC}, H_{LC}, H_{UM} (kJ mol^{-1})	141, 238, 445	219, 276, 535

s^{-1}) when plate boundaries are concerned. This last range has been adopted for strain rate in computing plastic flow stress by eq. (2.6).

Studies of the thermal evolution of mountain belts (*e.g.*, Midgley and Blundell, 1997; Liu, 2001) predict that immediately after the cessation of orogenesis the geotherm has a sawtooth shape, due to the stacking of crustal thrust sheets. Heat production induced by thrust shearing and decay of radioactive isotopes induces a thermal relaxation lasting millions of years after orogenesis. The final point of this process is the steady-state conductive geotherm (Chapman, 1986) we assume to hold through the whole lithosphere.

This kind of temperature-depth relationship depends on lithological layering, surface heat flow and thermal parameters of rocks. For a homogeneous layer we have

$$t(z) = -\frac{Qz^2}{2k} + \frac{q_0 z}{k} + t_0 \qquad (2.7)$$

where t, t_0, q_0, k, Q are the temperature at depth z, surface temperature, surface heat flow, average thermal conductivity and heat production per unit volume, respectively. To obtain a more realistic geotherm, eq. (2.7) may easily be adapted to a layered crust (*e.g.*, Ranalli and Murphy, 1987; Viti *et al.*, 1997).

The uncertainty that may affect the thermal parameters k and Q depends on the uncertainty about the composition of each crustal layer. To take this variability into account we have considered the upper and lower bounds of available experimental values of the above thermal parameters (tables I and II).

2.4. *Resistance at underthrusting boundaries*

Interplate coupling contributes to laterally sustain the thickened crust (*e.g.*, Platt, 1986). At an underthrusting boundary (subduction or collision), we define the resistance per unit length as

$$T = \Delta\sigma_{UN} L = 2\tau L \qquad (2.8)$$

where $\Delta\sigma_{UN}$ is the stress difference related to the the average frictional strength (τ) at the contact between the accretionary belt and the underthrusting crust and L is the down-dip length of this subduction fault (fig. 2). Basic rock mechanics (*e.g.*, Jaeger and Cook, 1984) shows that the lower bound of stress difference is twice the related shear stress, since $\tau = \Delta\sigma_{UN}(\sin 2\alpha/2)$, where α is the angle between the maximum principal stress σ_1 and the plane on which τ acts ($0 \le \alpha \le \pi/2$). To obtain a conservative estimate of T, we adopt the above bound for $\Delta\sigma_{UN}$ in eq. (2.8).

Quantifications of the average frictional strength, mostly based on estimates of frictional heating, indicate that a realistic range for τ is 14-43 MPa for subduction faults (Tichelaar and Ruff, 1993) and 25-50 MPa for continental thrusts (England and Molnar, 1991). The limits of the above intervals have been used to obtain realistic bounds of T. The length L has tentatively been estimated at each boundary from crustal sections reconstructed by seismic surveys, whose references are given in table I.

3. Assessment of tectonic forces in orogenic belts

To estimate the force balance related to crustal collapse for the eight orogenic belts considered (fig. 1a-c), we have collected structural and heat flow data by taking into account the most up-to-date geophysical evidence (table I). However, as discussed in the following sections, a reliable assessment of the feasibility of the gravitational collapse must take into account the level of uncertainty that may affect the estimate of the spreading and resisting forces.

3.1. *Constraining spreading force*

The uncertainty on the spreading force is mainly conditioned by the approximate knowledge we have on the density depth-distribution (*e.g.*, Rey and Costa, 1999). Taking into account the density ranges currently suggested for the upper crust, lower crust and lithospheric mantle (table II), we have defined two density distributions, hereinafter identified as «Low Density» (*LD*) and «High Density» (*HD*) models respectively (table III). In the *LD* model, the lower bounds of the density ranges reported in table II have been assigned to the chain, and the upper bounds to the foreland or the subducting plate. The opposite combination of density values has instead been adopted for the *HD* model. Then, an estimate of the lower and upper bound of the spreading force has been obtained using the above *LD* and *HD* density models in eq. (2.2), respectively.

3.2. *Constraining crustal strength*

Since thermal and rheological parameters strongly depend on rock type (table II), uncer-

tainty on crustal lithology considerably affects the estimate of the plastic flow stress by eq. (2.6), which in turn affects the integrated crustal strength defined by eqs. ((2.3a) and (2.3b)). To tentatively assess the above uncertainty, we have considered two combinations of thermal and rheological parameters, here indicated as the «Low Strength» (*LS*) and «High Strength» (*HS*) models (table III), chosen among the values reported in literature (table II). In the *LS* model, the plastic flow stress of the upper and lower crust is respectively controlled by the rheological parameters of granite and anorthosite. The thermal conductivity and heat production related to these rock types respectively correspond to the lower and upper bound of the ranges reported in table II. For this model we have also assumed the maximum value of surface heat flow, among those estimated in the orogenic belts (table I), and the lowest value of strain rate. In the *HS* model, the representative rocks for the upper and lower crust are quartzdiorite and diabase, respectively. The thermal conductivity and heat production of these rocks respectively corresponds to the upper and lower bounds of the proposed ranges (table II). For this model we assumed the minimum value of surface heat flow (table I) and the highest value of strain rate. The *LS* and *HS* models may be taken as lower and upper bounds for the tensional strength of the chain (*R*) and for the compressional strength of the foreland (*C*).

To estimate the lower and upper bounds of the resisting force at subduction/underthrusting boundaries (*T*) by eq. (2.8), we have adopted the ranges of fault shear strength reported in table II.

4. Results

Taking into account the structural parameter (topographic height and thickness of crustal layers) for the chain, foreland and subducting/underthrusting plate (table I), along with the relevant density model (table III), we have computed by eq. (2.2) the lower and upper bounds of the spreading forces acting on both sides of the belt (table IV).

Structural data (table I), along with the proposed combinations of thermal and rheological parameters (table III), have also been used for determining the lithospheric geotherm (eq. (2.7)) and the integrated strength of the various domains [eqs. ((2.3a) and (2.3b))]. The rock strength values, computed by eq. (2.4) using both *LS* and *HS* models, have been plotted with respect to depth to obtain the tensional strength envelopes of the chain for the various orogenic belts (fig. 4). These envelopes show that when the *LS* model is adopted, the lower crust is always ductile ($\Delta\sigma_T = \Delta\sigma_{PL}$) and much weaker than the underlying mantle. This may allow the crust to decouple from mantle and laterally flow under a spreading force which depends on lateral variation of crustal thickness, as we have assumed in computing *F* by eq. (2.2). Moreover, adopting the *LS* model implies negligible mechanical strength at the upper/lower crust boundary (fig. 4). On the other hand, when the *HS* model is considered, the crust is considerably less decoupled from upper mantle, which makes more difficult its eventual lateral flow by gravity spreading. However, in three cases (Tibetan Plateau, Altiplano and Lepontine Alps in fig. 4), the rock strength predicted at the crust-mantle boundary is negligible for both the *LS* and *HS* models, which implies complete decoupling and possibility of lateral flow of crust. Adopting the *HS* model also implies significant strength at the upper/lower crust boundary, so that in some cases (Calabria, Sierra nevada, Crete, Colorado Plateau and Umbria-Marche belt in fig. 4) the whole crust appears brittle/semibrittle with no internal decoupling.

Table IV reports the upper and lower bound of the tensional strength of the chain (*R*), the compressional strength of the foreland (*C*) and the strength of the interplate boundary (*T*), obtained by eqs. ((2.3a), (2.3b) and (2.8)), respectively. Spreading force and resistances have been computed for the two possible models of gravitational collapse here considered, one involving the upper crust only (fig. 5a,b) and the other involving the whole crust (fig. 6a,b). For each model, according to the sketch shown in fig. 2, both the cases that spreading occurs towards the underthrusting plate or towards the foreland has been investigated.

The results obtained (table IV; figs. 5a,b and 6a,b) show that the uncertainty on rock density, thermal parameters and rheological properties

produce a considerable scattering of the values related to driving and resisting forces. In figs. 5a,b and 6a,b the force balance for each orogenic belt, described by eq. (2.1), is constrained by the upper and lower bounds computed for the spreading force (F) and the mechanical strength of the crust ($R+T$ and $R+C$, respectively). These bounds are the vertices of the rectangular box that confines the possible combinations of driving force and resistances.

The main features of the the above diagrams can be summarized as follows:

1) For the Mediterranean orogenic belts here considered, *i.e.* Northern Apennines, Calabrian Arc, Hellenic Arc and Carpathians, the feasibility of the collapse model, both concerning the upper and whole crust, can reasonably be ruled out. For the Central Alps, gravitational collapse may be considered unlikely, even if it cannot be completely ruled out.

2) For the Western US Cordillera the force balance is more uncertain. Collapse of Sierra Nevada towards its western foreland (Great Valley in fig. 1a-c) does not seem to be feasible, whereas spreading of Sierra Nevada and Colorado Plateau towards the Great Basin cannot be ruled out (figs. 5b and 6b).

3) For the other zones, *i.e.* Himalayas and Central Andes, the uncertainty on the various terms of the force balance does not allow drawing a firm conclusion about the feasibility of gravitational collapse. In any case, for these belts the collapse of the upper crust (fig. 5a,b) seems to be more unlikely than that of the

Table IV. Average spreading (F) and resisting (R, C and T) forces computed for the 8 orogenic belts considered in this work. All the values are expressed as force per unit length of the orogenic belt; the scale factor being 10^{12} Nm^{-1}. The bounding values of forces reported in the table have been obtained by taking into account the combinations of physical parameters shown in table III. Results are provided for the collapse of the upper crust (upper row of each box) and of the whole crust (lower row). Symbols and geographical names as in figs. 1a-c, 2 and table I.

Western US Cordillera 1		
F	*R*	*C*
Towards Great Valley	Sierra Nevada	Great Valley
1.5-1.9	0.5-2.8	2.1-4.9
2.4-4.8	1.4-9.9	5.6-9.4
F		*C*
Towards Great Basin		Great Basin
0.8-1.2		0.4-4.8
0.9-3.2		0.5-9.6
Western US Cordillera 2		
F	*R*	*C*
Towards Great Basin	Colorado Plateau	Great Basin
0.3-0.9	0.2-4.6	0.4-2.5
0.4 -1.5	0.3-8.8	0.5-6.1
Central Andes		
F	*R*	*C*
Towards Chaco Basin	Altiplano	Chaco Basin
2.5-2.9	0.1-2.9	2.2-10.1
5.7-11.3	0.2-4.4	3.5-13.1
F		*T*
Towards Pacific Ocean		Nazca/S. America
3.5-3.9		4.2-13.
4.6-10.		

Table IV (*continued*)**.**

Himalayas		
F Towards Ordos Basin 2.1-2.6 2.8-9.3	*R* Tibetan Plateau 0.2-3.5 0.3-5.5	*C* Ordos Basin 1.1-6.5 1.6-13.6
F Towards Gange Basin 2.6-3.0 4.-10.5		*T* India/Eurasia 8.-16.
Central Alps		
F Towards Molasse Basin 1.-1.9 1.1-3.2	*R* Lepontine Alps 0.3-4.5 0.4-6.8	*C* Molasse Basin 0.5-6.6 0.6-8.9
F Towards Po Basin 1.4-2.2 1.5-4.		*T* Adriatic/Eurasia 6.2-12.4
Northern Apennines		
F Towards Northern Tyrrhenian Basin 0.3-0.5 0.4-1.3	*R* Umbria-Marche Belt 0.6-1.6 4.0-7.3	*C* N. Tyrrhenian Basin 0.2-3.7 0.3-6.7
F Towards Adriatic Basin 0. 3-0.5 0.4-1.9		*T* Adriatic/Apennines 5.-10.
Calabrian Arc		
F Towards Southern Tyrrhenian Basin 1.1-1.5 1.2-1.8	*R* Calabria 0.6-2.8 2.4-4.5	*C* S. Tyrrhenian Basin 1.3-2.5 1.4-2.6
F Towards Ionian Basin 1.6-1.9 2.-2.5		*T* Africa/Calabria 3.4-10.2
Hellenic Arc		
F Towards Cretan Basin 0.8-0.9 1.1-2.3	*R* Crete 0.6-1.2 3.8-6.7	*C* Cretan Basin 1.-1.2 1.2-1.3
F Towards Herodotus Basin 1.0-1.1 2.8-3.8		*T* Africa/Crete 4.2-13.

Table IV (*continued*)**.**

Carpathians		
F	*R*	*C*
Towards Transylvanian Basin	Southeastern Carpathians	Transylvanian Basin
0.2-0.7	0.4-1.3	1.7-3.7
0.3-1.8	1.0-10.2	5.3-9.1
F		*T*
Towards Moesian Platform		Moesia/Carpathians
0.3-0.7		9.-18.
0.4-1.9		

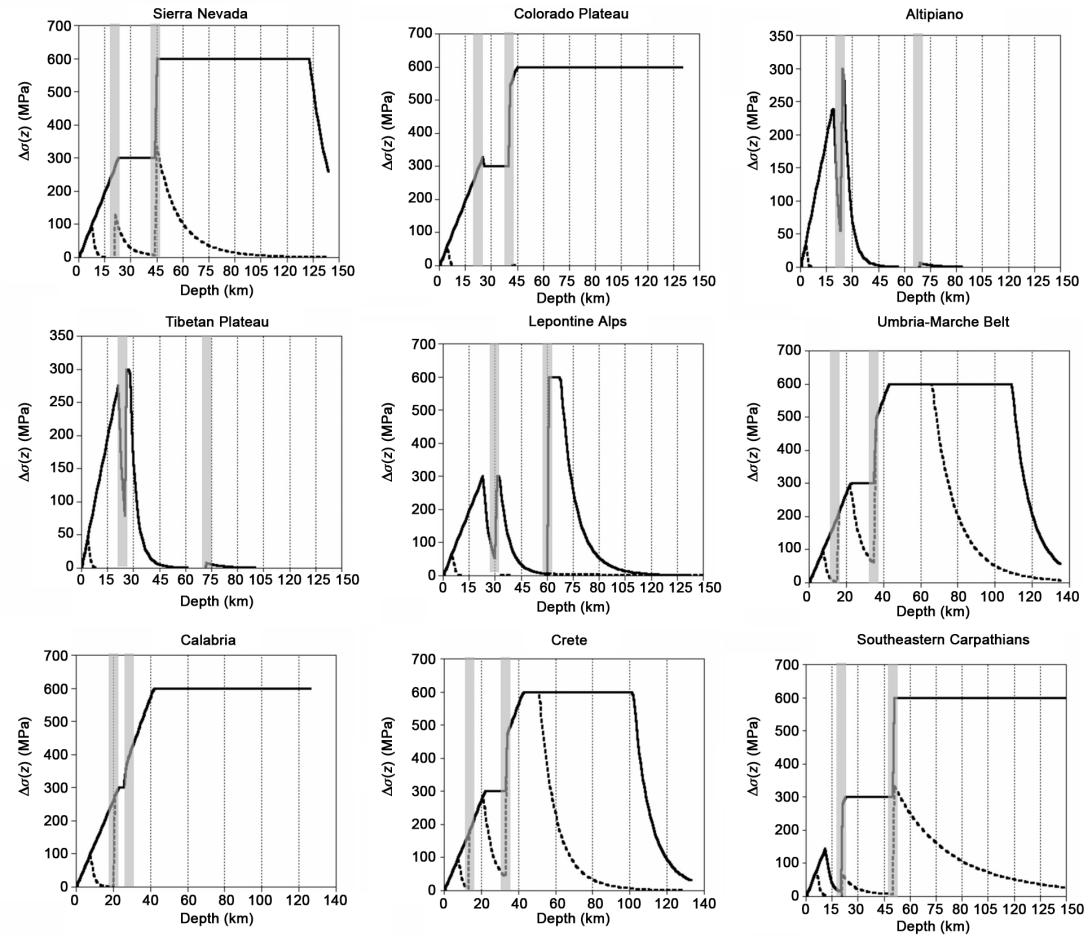

Fig. 4. Strength envelopes of the chain for the orogenic belts considered in this work. The function $\Delta\sigma(z)$ has been used to compute the integrated tensional strength R by (2.3a). The dotted and solid curves are the $\Delta\sigma(z)$ relationships obtained adopting the *LS* and *HS* strength model, respectively (see table III and text for explanations). The grey strips indicate the upper/lower crust and crust/mantle boundaries. Geographical names as in fig. 1a-c and table I.

whole crust (fig. 6a,b), for which much higher spreading forces are predicted.

It is appropriate to recall that in three orogenic belts only (Altiplano, Tibetan Plateau and Lepontine Alps in fig. 4) the complete mechanical decoupling between crust and mantle results possible, no matter the strength model (*i.e.* the above *LS* and *HS* ones) adopted in recostructing the rheological profile. Taking into account this last features and the results on force balance discussed above, it is seems reasonable to conclude that at most gravitational spreading might be a feasible driving mechanism for the two thickest orogenic belts here considered: Central Andes and Himalayas.

5. Discussion and conclusions

Significant insights into the feasibility of gravitational spreading in a thickened zone may only be obtained by taking into account the specific structural, thermal and rheological features of the structural system involved. Since these features are poorly constrained for most of the orogenic zones here considered, the various terms of the force balance may be affected by a large uncertainty. In spite of this, the results of our analysis allow stating that crustal collapse is not a plausible mechanism for the Mediterranean orogenic belts (Northern Apennines, Calabrian Arc, Hellenic Arc and Carpathians). No definitive conclusion can be drawn, instead, for the Western US Cordillera, Central Andes, Himalayas and Central Alps.

It must be pointed that the above conclusions are only tentative, since the approach adopted for the computation of the force balance is over-simplified in many respects. In particular, our choices about structural model of orogenic belts, crustal geotherm and force balance deserves some comments.

We have assumed that the value of the quantity *F*, obtained from the available thermal and structural data, appropriately represents the average spreading force acting on the whole belt.

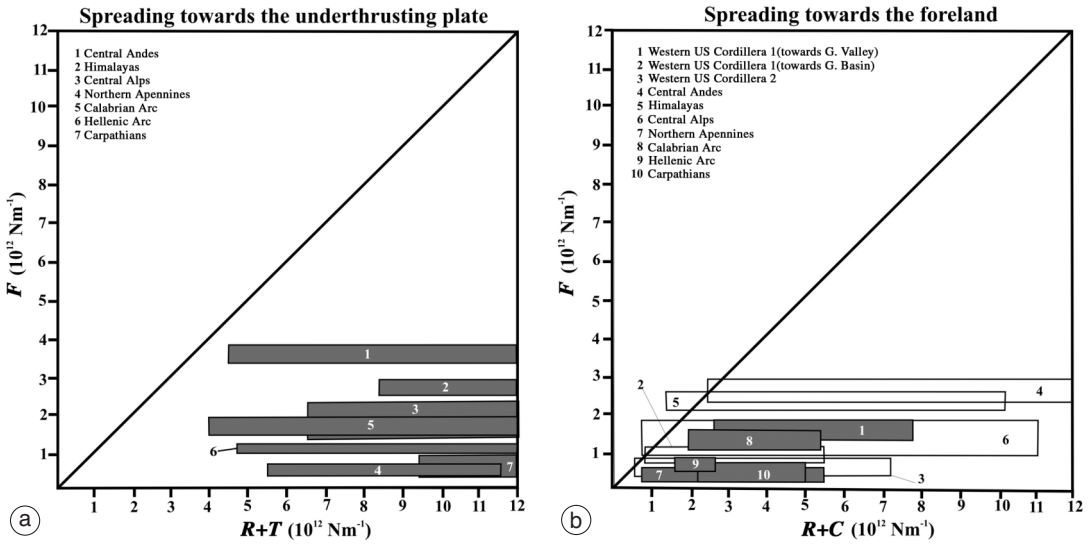

Fig. 5a,b. Diagrams of the force balance in the case of collapse of the upper crust. Rectangular boxes indicate the ranges of the spreading (*F*) and resisting forces (*R+T, R+C*) computed for the 8 belts considered (table IV). The diagonal thick line correspond to the equilibrium between the spreading force and the sum of resistances. Grey indicates the cases for which the sum of resistances overcomes the spreading force (see text for details).

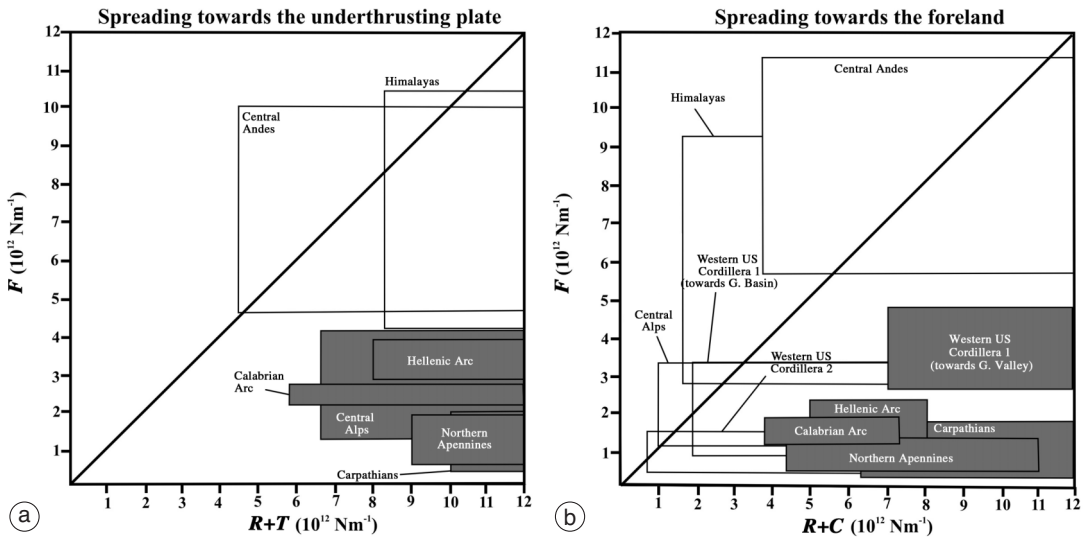

Fig. 6a,b. Force balance when the collapse involves the whole crust (see caption of fig. 5a,b and text for details).

Since these data refer to few cross sections for each belt considered, the three-dimensional structure of the orogenic system is very approximately simulated. However, it is also true that the values reported in table I refer to the central zone of the various mountains belts, where the largest variations of crustal thickness and heat flow occur. Thus, the value of F we have computed for each belt reasonably represents an upper bound of the values that could be obtained by considering more peripheral sectors of that orogenic system. Analogous arguments can be advanced to justify our choice of estimating crustal strength along cross sections. This choice implies that the adopted values refer to the thickest and hottest zone of the belt, and that, consequently, the resulting value may be taken as a lower bound of R.

Finally, the force balance described by eq. (2.1) could be extended to other terms, such as ridge push and slab pull, which might influence the occurrence of gravitational collapse. However, these forces and the related uncertainties are not easily estimable for the orogenic systems here considered, since the physical parameters of spreading ridges and subducting slabs involved are known very approximately. Thus, we have not included the above terms in the force balance. In any case, numerical modelling has shown that compressional forces induced by plate convergence act against the tensional stress generated by lateral variations of crustal thickness (*e.g.*, England and Houseman, 1989; Richardson and Coblentz, 1994).

Numerical modelling (*e.g.*, England and Houseman, 1989*;* Liu *et al.*, 2000; Liu and Yang, 2003) can be used to investigate the plausibility of gravitational collapse in the orogenic belts we have considered. However, our simplified approach allows a relatively easy assessment of the uncertainty that may affect the driving and resisting forces controlling gravitational collapse. This may be useful as a preliminary step in the elaboration of a numerical model. On the other hand, overlooking the above uncertainties would make almost useless any attempt to model gravitational collapse.

Acknowledgements

We would like to thank M.E. Belardinelli and S. Santini, whose comments have significantly improved our work.

REFERENCES

ANDREESCU, M., S. B. NIELSEN, G. POLONIC and C. DEMETRESCU (2002): Thermal budget of the Transylvanian lithosphere. Reasons for a low surface heat-flux anomaly in a Neogene intra-Carpathian Basin, *Geophys. J. Int.*, **150**, 494-505.

BASSI, G. (1995): Relative importance of strain rate and rheology for the mode of continental extension, *Geophys. J. Int.*, **122**, 195-210.

BIRD, P. (1991): Lateral extrusion of lower crust from under high topography, in the isostatic limit, *J. Geophys. Res.*, **96**, 10275-10286.

BIRD, P. (2002): Stress direction history of the Western United States and Mexico since 85 Ma, *Tectonics*, **21**, 5/1-12, doi:10.1029/2001TC001319.

BOHNHOFF, M., J. MAKRIS, D. PAPANIKOLAU and G.N. STAVRAKAKIS (2001) Crustal investigation of the Hellenic subduction zone using wide aperture seismic data, *Tectonophysics*, **343**, 239-262.

BUROV, E.B. (2003): The upper crust is softer than dry quartzite, *Tectonophysics,* **361***,* 321-326.

BYERLEE, J.D. (1978): Friction of rocks, *Pure Appl. Geophys.*, **116**, 615-626.

CARISTAN, Y. (1982): The transition from high temperature creep to fracture in Maryland diabase, *J. Geophys. Res.*, **87**, 6781-6790.

CARMIGNANI, L., F.A. DECANDIA, P.L FANTOZZI, A. LAZZAROTTO, D. LIOTTA and M. MECCHERI (1994): Tertiary extensional tectonics in Tuscany (Northern Apennines, Italy), *Tectonophysics*, **238**, 295-315.

CATALDI, R., F. MONGELLI, P. SQUARCI, L. TAFFI, G. ZITO and C. CALORE (1995): Geothermal ranking of italian territory, *Geothermics,* **24**, 115-129.

CATTIN, R., G. MARTELET, P. HENRY, J.P. AVOUAC, M. DIAMENT and T.R. SHAKYA (2001): Gravity anomalies, crustal structure and thermo-mechanical support of the Himalaya of Central Nepal, *Geophys. J. Int.*, **147**, 381-392.

CERMAK, V. (1993): Lithospheric thermal regimes in Europe, *Phys. Earth planet. Interiors*, **79**, 179-193.

CERMAK, V. and L. BODRI (1996): Time-dependent crustal temperature modeling: Central Alps, *Tectonophysics*, **257**, 7-24.

CHAPMAN, D.S. (1986): Thermal gradients in the continental crust, in *The Nature of the Lower Continental Crust*, edited by J.B. DAWSON, D.A. CARLSWELL, J. HALL and K.H. WEDEPOHL, *Geol. Soc. London Spe. Publ.*, **24**, 63-70.

CHOPRA, P.N. and M.S. PATERSON (1984): The role of water in the deformation of dunites, *J. Geophys. Res.*, **89**, 7861-7876.

CHRISTENSEN, N.I. and W.D. MOONEY (1995): Seismic velocity structure and composition of the continental crust: a global view, *J. Geophys. Res.*, **100**, 9761-9788.

COBLENTZ, D.D. and M. SANDIFORD (1994): Tectonic stresses in the African plate: constraints on the ambient lithospheric stress state, *Geology*, **22**, 831-834.

DALMAYER, B. and P. MOLNAR (1981): Parallel thrust and normal faulting in Peru and constraints on the state of stress, *Earth planet. Sci. Lett.*, **55**, 473-481.

DE VOOGD, B., C. TRUFFERT, N. CHAMOT-ROOKE, P. HUCHON, S. LALLEMANT and X. LE PICHON (1992): Two-ship deep seismic soundings in the basins of the Eastern Mediterranean Sea (Pasiphae cruise), *Geophys. J. Int.*, **109**, 536-552.

DELLA VEDOVA, B., F. LUCAZEAU, V. PASQUALE, G. PELLIS and M. VERDOYA (1995): Heat flow in the tectonic provinces crossed by the southern segment of the European geotraverse, *Tectonophysics*, **244**, 57-74.

DEWEY, J.F. (1988): Extensional collapse of orogens, *Tectonics*, **7**, 1123-1139.

DUSCHENES, J. and M.C. SINHA (1986): A seismic refraction experiment in the Tyrrhenian Sea, *Geophys. J. Int.*, **85**, 139-160.

ENGLAND, P. and G.A. HOUSEMAN (1988): The mechanics of the Tibetan Plateau, *Philos. Trans. R. Soc. London*, **326**, 301-319.

ENGLAND, P. and G.A. HOUSEMAN (1989): Extension during continental convergence, with application to the Tibetan Plateau, *J. Geophys. Res.*, **94**, 17561-17579.

ENGLAND, P. and P. MOLNAR (1991): Inferences of deviatoric stresses in actively deforming belts from simple physical models, *Philos. Trans. R. Soc. London.*, **337**, 151-164.

EVA, E. and S. SOLARINO (1998): Variations of stress directions in the Western Alpine Arc, *Geophys. J. Int.*, **135**, 438-448.

FAN, G., T.C. WALLACE and D. ZHAO (1998): Tomographic imaging of deep velocity structure beneath the Eastern and Southern Carpathians, Romania: implications for continental collision, *J. Geophys. Res.*, **103**, 2705-2723.

FERNÀNDEZ, M. and G. RANALLI (1997): The role of rheology in extensional basin formation modelling, *Tectonophysics*, **282**, 129-145.

FINETTI, I.R., M. BOCCALETTI, M. BONINI, A. DEL BEN, R. GELETTI, M. PIPAN and F. SANI (2001): Crustal section based on CROP seismic data across the North Tyrrhenian-Northern Apennines-Adriatic Sea, *Tectonophysics*, **343**, 135-163.

FLIEDNER, M.M., N.I. KLEMPERER and N.I. CHRISTENSEN (2000): Three-dimensional seismic model of the Sierra Nevada arc, California, and its implications for crustal and upper mantle composition, *J. Geophys. Res.*, **105**, 10899-10921.

FLUEH, E.R., N. VIDAL, C.R. RANERO, A. HOJKA, R. VON HUENE,, J. BIALAS, K. HINZ, D. CORDOBA, J.J. DAÑOBEITIA and C. ZELT (1998): Seismic investigation of the continental margin off- and onshore Valparaiso, Chile, *Tectonophysics*, **288**, 251-263.

GAUTIER, P., J.-P. BRUN, R. MORICEAU, D. SOKOUTIS, J. MARTINOD and L. JOLIVET (1999): Timing, kinematics and cause of Aegean extension: a scenario based on a comparison with simple analogue experiments, *Tectonophysics*, **315**, 31-72.

GIESE, P., E. SCHEUBER, F. SCHILLING, M. SCHMITZ and P. WIGGER (1999): Crustal thickening processes in the Central Andes and the different natures of the Moho-discontinuity, *J. South Am. Earth Sci.*, **12**, 201-220.

GIUDICI, M. and L. GUALTERI (1998): Application of revised ray tracing migration to imagine lateral variations of seismic fabric corresponding to different tectonic styles in the Northern Apennines, *Tectonophysics*, **300**, 181-197.

GOETZE, C. and B. EVANS (1979): Stress and temperature in the bending lithosphere as constrained by experimental rock mechanics, *Geophys. J. R. Astron. Soc.*, **59**, 463-468.

GUALTERI, L., G. BERTOTTI and S. CLOETINGH (1998): Lateral variations of thermo-mechanical properties in the Tyrrhenian-Northern Apennines region, *Tectonophysics*, **300**, 143-158.

HANSEN, F.D. and N.L. CARTER (1982): Creep of selected rocks at 1000 MPa, *Eos, Trans. Am. Geophys. Un.*, **63**, 437.

HARRY, D.L., D.S. SAWYER and W.P. LEEMAN (1993): The mechanics of continental extension in western North America: implications for the magmatic and structural evolution of the Great Basin, *Earth Planet. Sci. Lett.*, **117**, 59-71.

HENK, A. (2002): Did the Variscides collapse or were they torn apart? A quantitative evaluation of the driving forces for postconvergent extension in Central Europe, *Tectonics,* **18***,* 774-792.

HINOJOSA, J.H. and K.L. MICKUS (1999): Thermoelastic modeling of lithospheric uplift: a finite-difference numerical solution, *Comput. Geosci.*, **28**, 155-167.

HU, S., L. HE and J. WANG (2000): Heat flow in the continental area of China: a new data set, *Earth Planet. Sci. Lett.*, **179**, 407-419.

ISACKS, B.L. (1988): Uplift of the Central Andean plateau and bending of the Bolivian orocline, *J. Geophys. Res.*, **93**, 3211-3231.

JAEGER, J.C. and N.G.W. COOK (1984): *Fundamentals of Rock Mechanics* (Chapman and Hall, New York), pp. 593.

JONES, C.H., L.J. SONDER and J.R. UNRUH (1998): Lithospheric gravitational potential energy and past orogenesis: implications for conditions of initial Basin and Range and Laramide deformation, *Geology*, **26**, 639-642.

JONES, C.H., J.L. SONDER and J.R. UNRUH (1999): Reply on «Lithospheric gravitational potential energy and past orogenesis: implications for conditions of initial basin and range and Laramide deformation», *Geology*, **27**, 475-476.

KAYAL, J.R. (2001): Microearthquake activity in some parts of the Himalaya and the tectonic model, *Tectonophysics*, **339**, 331-351.

KOHLSTEDT, D.L., B. EVANS and S.J. MACKWELL (1995): Strength of the lithosphere: constraints imposed by laboratory experiments, *J. Geophys. Res.*, **100**, 17587-17602.

LINZER, H.-G., W. FRISCH, P. ZWEIGEL, R.GIRBACEA, H.-P. HANN and F. MOSER (1998): Kinematic evolution of the Romanian Carpathians, *Tectonophysics*, **297**, 133-156.

LIU, M. (2001): Cenozoic extension and magmatism in the North American Cordillera: the role of gravitational collapse, *Tectonophysics*, **342**, 407-433.

LIU, M. and Y. SHEN (1998): Crustal collapse, mantle upwelling, and Cenozoic extension in the North America Cordillera. *Tectonics*, **17**, 311-321.

LIU, M. and Y. YANG (2003): Extensional collapse of the Tibetan Plateau: Results of three-dimensional finite element modeling, *J. Geophys. Res.*, **108**, 2361, ETG2/1-15, doi: 10.1029/2002JB002248.

LIU, M., Y. SHEN and Y. YANG (2000): Gravitational collapse of orogenic crust: a preliminary three-dimensional finite element study, *J. Geophys. Res.*, **105**, 3159-3173.

LOWRY, A.R. and R.B. SMITH (1995): Strength and rheology of the Western US Cordillera, *J. Geophys. Res.*, **100**, 17947-17963.

LUCASSEN, F., R. BECCHIO, R. HARMON, S. KASEMANN, G. FRANZ, R. TRUMBULL, H.-G. WILKE, R.L. ROMER and P. DULSKI (2001): Composition and density model of the continental crust at an active continental margin-the Central Andes between 21° and 27°S, *Tectonophysics*, **341**, 195-223.

MANTOVANI, E., M. VITI, D. BABBUCCI, C. TAMBURELLI and D. ALBARELLO (2001): Back arc extension: which driving mechanism?, *J. Virtual Explorer*, **3**, 17-44.

MANTOVANI, E., D. ALBARELLO, D. BABBUCCI, C. TAMBURELLI and M. VITI (2002): Trench-Arc-Back-Arc systems in the Mediterranean area: examples of extrusion tectonics, in *Reconstruction of the Evolution of the Alpine-Himalayan Orogen*, edited by G. ROSENBAUM and G. LISTER, *J. Virtual Explorer*, **8**, 131-147.

MANTOVANI, E., M. VITI, D. BABBUCCI, C. TAMBURELLI and D. ALBARELLO (2006): Geodynamic connection between the indentation of Arabia and the Neogene tectonics of the central-eastern Mediterranean region, in *Post-Collisional Tectonics and Magmatism in the Easterm Mediterranean Region*, edited by Y. DILEK and S. PAVLIDES, *Geol. Soc. America Special Papers*, **409**, 15-41.

MAGGI, A., J.A. JACKSON, D. MCKENZIE and K. PRIESTLEY (2000): Earthquake focal depths, effective elastic thickness, and the strength of the continental lithosphere, *Geology*, **28**, 495-498.

MARCHANT, R.H. and G.M. STAMPFLI (1997): Subduction of continental crust in the Western Alps, *Tectonophysics*, **269**, 217-235.

MEISSNER, R. and W. MOONEY (1998): Weakness of the lower continental crust: a condition for delamination, uplift, and escape, *Tectonophysics,* **296**, 47-60.

MIDGLEY, J.P. and D.J. BLUNDELL (1997): Deep seismic structure and thermo-mechanical modelling of continental collision zones, *Tectonophysics*, **273**, 155-167.

MOLNAR, P. and H. LYON-CAEN (1988): Some simple physical aspects of the support, structure and evolution of mountain belts, *Geol. Soc. Am. Spec. Pap.*, **218**, 179-207.

MUELLER, S., G.L. CHOY and W. SPENCE (1996): Inelastic models of lithospheric stress-I. Theory and application to outer-rise plate deformation, *Geophys. J. Int.*, **125**, 39-53.

OKAYA, N., S. CLOETINGH and ST. MUELLER (1996): A lithospheric cross-section through the Swiss Alps-II. Constraints on the mechanical structure of a continent-continent collision zone, *Geophys. J. Int.*, **127**, 399-414.

ORD, A. (1991): Deformation of rock: a pressure-sensitive, dilatant material, *Pure appl. Geophys.*, **137**, 337-366.

PASQUALE, V., M. VERDOYA, P. CHIOZZI and G. RANALLI (1997): Rheology and seismotectonic regime in the northern central Mediterranean, *Tectonophysics*, **270**, 239-257.

PELTZTER, G. and F. SAUCIER (1996): Present-day kinematics of Asia derived from geologic fault rates*, J. Geophys. Res.,* **101***,* 27943-27956.

PFIFFNER, A. and J.G. RAMSAY (1982): Constraints on geological strain rates: arguments from finite-strain states of naturally deformed rocks, *J. Geophys. Res.*, **87**, 311-321.

PLATT, J.P. (1986): Dynamics of orogenic wedges and the uplift of high-pressure metamorphic rocks, *Geol. Soc. Am. Bull.*, **97**, 1106-1121.

POIRIER, J.-P. (2005): *Creep of Crystals* (Cambridge University Press), pp. 260.

PONZIANI, F., R. DE FRANCO, G. MINELLI, G. BIELLA, C. FEDERICO and G. PIALLI (1995): Crustal shortening and duplication of the Moho in the Northern Apennines: a view from seismic refraction data, *Tectonophysics*, **252**, 391-418.

RANALLI, G. (1997): Rheology of the lithosphere in space and time, in *Orogeny Through Time*, edited by J.-P. BURG and M. FORD, *Geol. Soc. London Spec. Publ.*, **121**, 19-37.

RANALLI, G. (2003): How soft is the crust?, *Tectonophysics,* **361**, 319-320.

RANALLI, G. and D.C. MURPHY (1987): Rheological stratification of the lithosphere, *Tectonophysics*, **132**, 281-295.

REY, P.F. and S. COSTA (1999): Comment on «Lithospheric gravitational potential energy and past orogenesis: implications for conditions of initial Basin and Range and Laramide deformation», *Geology*, **27**, 475.

REY, P.F., O. VANDERHAEGHE and C. TEYSSIER (2001): Gravitational collapse of the continental crust: definition, regimes and modes, *Tectonophysics*, **342**, 435-449.

RICHARDSON, R.M. and D.D. COBLENTZ (1994): Stress modeling in the Andes: constraints on the South America intraplate stress magnitude, *J. Geophys. Res.*, **99**, 22015-22025.

RUPPERT, S., M.M. FLIEDNER and G. ZANDT (1998): Thin crust and active upper mantle beneath the Southern Sierra Nevada in the Western United States, *Tectonophysics*, **286**, 237-252.

SATARUGSA, P. and R.A. JOHNSON (2000): Constraints on crustal composition beneath a metamorphic core complex: results from 3-component wide-angle seismic data along the eastern flank of the Ruby Mountains, Nevada, *Tectonophysics*, **329**, 223-250.

SCHMITZ, M., K. LESSEL, P. GIESE, P. WIGGER, M. ARANEDA, J. BRIBACH, F. GRAEBER, S. GRUNEWALD, C. HABERLAND, S. LÜTH, P. RÖWER, T. RYBERG and A. SCHULZE (1999): The crustal structure beneath the Central andean forearc and magmatic arc as derived from seismic studies – The PISCO 94 experiment in Northern Chile (21°-23°S), *J. South Am. Earth Sci.*, **12**, 237-260.

SERBAN, D.Z., S.B. NIELSEN and C. DEMETRESCU (2001): Transylvanian heat flow in the presence of topography, paleoclimate and groundwater flow, *Tectonophysics*, **335**, 331-344.

SHELTON, G. and J.A. TULLIS (1982): Experimental flow laws for crustal rocks, *Eos, Trans. Am. Geophys. Un.*, **62**, p. 396.

SHIMADA, M. (1993): Lithosphere strength inferred from fracture strength of rocks at high confining pressures and temperatures, *Tectonophysics*, **217**, 55-64.

SMITH, R.B. and R.L. BRUHN (1984): Intraplate extensional tectonics of the eastern Basin-Range: inferences on structural style from seismic reflection data, regional tectonics, and thermal-mechanical models of brittle-ductile deformation, *J. Geophys. Res.*, **89**, 5733-5762.

SPRINGER, M. and A. FÖRSTER (1998): Heat-flow density across the Central Andean subduction zone, *Tectonophysics*, **291**, 123-139.

TALWANI, P. (1999): Fault geometry and earthquakes in continental interiors, *Tectonophysics*, **305**, 371-379.

TICHELAAR, B.W. and L.J. RUFF (1993): Depth of seismic coupling along subduction zones, *J. Geophys. Res.*, **98**, 2017-2037.

VANDERHAEGHE, O. and C. TEYSSIER (2001): Partial melting and flow of orogens, *Tectonophysics,* **342***,* 451-472.

VAN DIJK, J.P., M. BELLO, G.P. BRANCALEONI, G. CANTARELLA, V. COSTA, A. FRIXA, F. GOLFETTO, S. MERLINI, M. RIVA, S. TORRICELLI, C. TOSCANO and A. ZERILLI (2000): A regional structural model for the northern sector of the Calabrian Arc (Southern Italy), *Tectonophysics*, **324**, 267-320.

VITI, M., D. ALBARELLO and E. MANTOVANI (1997): Rheological profiles in the central-eastern Mediterranean, *Ann. Geofis.*, **XL** (4), 849-864.

WANG, Y. (2001): Heat flow pattern and lateral variations of lithosphere strength in China mainland: constraints on active deformation, *Phys. Earth Planet. Inter.*, **126**, 121-146.

WANG, G. and R.J. MUNROE (1982): Heat flow and subsurface temperatures in the Great Valley, California, *Technical Rep. USGS-OFR-82-844* (Denver, U.S.A.), pp. 102.

WEERTMAN, J. (1978): Creep laws for the mantle of the Earth, *Philos. Trans. R. Soc. London A*, **288**, 9-26.

ZOBACK, M.D. and J. TOWNEND (2001): Implications of hydrostatic pore pressures and high crustal strength for the deformation of intraplate lithosphere, *Tectonophysics*, **336**, 19-30.

(received May 17, 2006;
accepted November 16, 2006)